The effect of femtosecond laser radiation on the optical surface of germanium

© I.A. Kaplunov[1], S.A. Tretiakov[1], A.I. Ivanova[1], A.D. Vasiliev[1], K.B. Yushkov[2], V.E. Rogalin[3]

[1] Tver State University,
170100 Tver, Russia
[2] National University of Science and Technology MISIS,
119049 Moscow, Russia
[3] Institute for Electrophysics and Electric Power, Russian Academy of Sciences,
191181 St. Petersburg, Russia

E-mail: kaplunov.ia@mail.ru

Received May 5, 2026
Revised June 26, 2026
Accepted July 3, 2026

The study of the effect of high-intensity radiation from a femtosecond laser with a wavelength of 1030 nm on the surface of germanium single crystals revealed the features of the resulting surface relief and patterns associated with different crystallographic orientation of the surfaces depending on the radiation power density and pulse repetition rate.

Keywords: germanium (Ge), crystallographic orientation, femtosecond laser, ablation, surface modification.

DOI: 10.61011/SC.2026.05.63994.9399

1. Introduction

Femtosecond lasers have become an established tool for a wide range of material processing applications [1–3] and are widely used in both scientific research and the manufacture of advanced products. Their advantages extend beyond the high power of pulsed radiation used to modify the surfaces of metals, semiconductors, and dielectrics and for many other applications. The short pulse duration minimizes the heat-affected zone, which is particularly important in semiconductor processing, especially cutting. Femtosecond laser pulses can be focused inside transparent optical materials, enabling three-dimensional (3D) micro- and nanomachining [4]. Femtosecond techniques also enable surface modification of opaque materials, where distinctive interaction effects likewise occur.

Single-crystal germanium was the material used to fabricate the first semiconductor integrated circuits. Ge was also found to have unique optical properties in the infrared (IR) spectral range [5]. Despite its high cost, Ge is in great demand for a variety of advanced applications.

This study examines the interaction of repetitive femtosecond laser pulses with the (100), (110), and (111) crystallographic surfaces of single-crystal germanium. Reference [6] investigated the formation of micro- and nanostructures on silicon using femtosecond laser radiation at wavelengths of 744 nm (100 fs pulse duration) and 248 nm (60 fs). The formation of craters and growing microcones on the silicon surface was shown to depend on the laser wavelength, exposure duration, number of pulses, and surface condition.

Creating a textured surface on single-crystal germanium can reduce reflectance and improve the efficiency of germanium-based photoelectric converters; surface modification can also be used to perform processing operations on optical element surfaces [5]. Given the expanding industrial applications of femtosecond laser systems, studying how radiation characteristics affect germanium surface modification is a relevant research objective.

2. Samples and experimental methods

The germanium samples were prepared from a single crystal grown by the Czochralski method, doped with antimony (resistivity $25-30\,\Omega\cdot$cm), and having a dislocation density of $(0.5-1.0)\cdot 10^4\,\mathrm{cm}^{-2}$. The samples were rectangular parallelepipeds with dimensions of $10\times 10\times 5$ mm. Samples with different crystallographic orientations were prepared; their polished 10×10 mm faces corresponded to the (100), (110), and (111) planes.

A fiber laser with a wavelength of 1030 nm ($\sigma = 330$ fs) and adjustable power and pulse repetition rate was used to investigate the effect of high-intensity radiation on germanium single-crystal surfaces. The radiation parameters were as follows: pulse repetition rate—100 kHz, average power —5 W, peak power —152 MW, and vertical polarization. The beam was focused onto the sample surface using a lens with a focal length of 300 mm, providing a beam waist diameter of 310 μm at the $1/e^2$ intensity level.

3. Results and discussion

The samples were irradiated at different locations (eight irradiation sites), varying the number of pulses per site; the exposure conditions are listed in Table 1. Figures 1 and 2 show measurements of the irradiated regions using a profilometer (NanoMap 1000WLI) and a scanning electron microscope (SEM; JEOL JSM 6610LV).

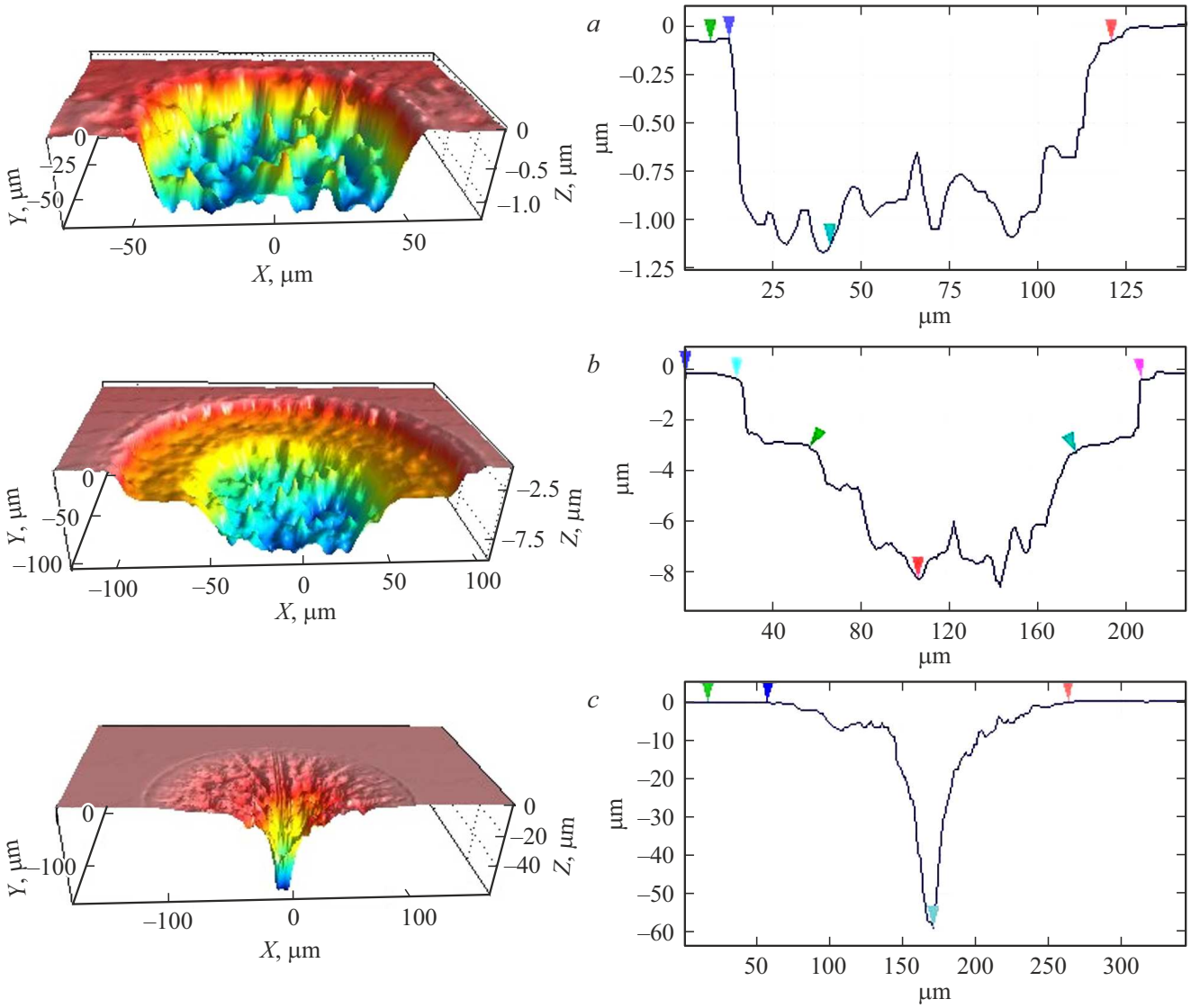


Figure 1. 3D and 2D crater profiles on germanium single crystals with a (100) surface orientation. Number of pulses: *a* — 10, *b* — 2000, *c* — 10 000.

Extensive datasets were collected (approximately 650 files covering 48 locations on the three samples at different magnifications and focal settings). Selected and averaged measurement results are presented here; the images show the irradiated surface with a (100) crystallographic orientation. Profilometry and scanning electron microscopy (SEM) of the pulsed-laser irradiation marks on samples with different crystallographic orientations revealed several trends. Profilometry, including surface analysis using the specialized software Gwyddion, provided averaged crater geometry data for different crystallographic directions (Table 2).

The (100) surface was found to be the most susceptible to damage: the craters formed on it were the deepest, and the Sa roughness of the crater floor was higher than for the other crystallographic planes. The crater diameters were comparable for all crystallographic orientations, since they are determined by ablation processes independent of crystallography. Crater formation involves the development of a polycrystalline grain structure in the near-surface

Table 1. Laser radiation parameters

Site №	Exposure time, ms	Number of pulses	Total energy, mJ
1	0.1	10	0.5
2	1	100	5
3	3	300	15
4	5	500	25
5	7	700	35
6	10	1000	50
7	20	2000	100
8	100	10000	500

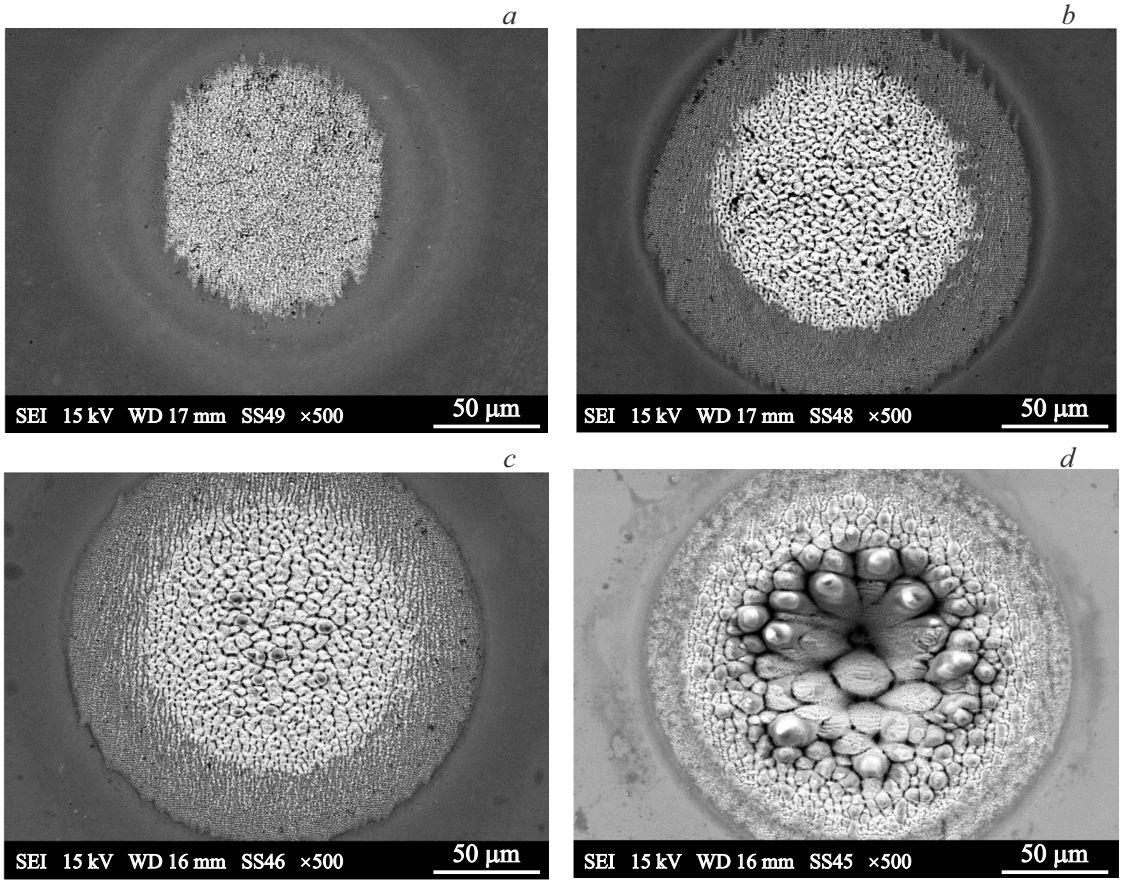


Figure 2. SEM images of craters on germanium single crystals with a (100) surface orientation. Number of pulses: *a* — 10, *b* — 300, *c* — 2000, *d* — 10 000.

germanium layer within the irradiated region, as well as the formation of channels inside the crater, visible in 2D profiles and SEM images. The crater diameter and depth vary with the number of pulses.

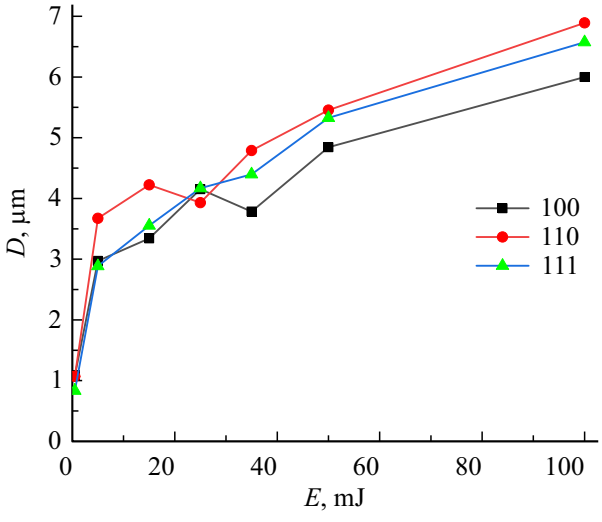


Figure 3. Grain dimensions following femtosecond laser irradiation as a function of the total energy in the pulse train.

The grains inside the craters formed by crystallization of the melt as it cooled between pulses and by deposition of germanium vapor. They contain substantial amounts of oxides with strongly nonequilibrium compositions. The grain size was found to depend on the energy in the pulse train and to increase with increasing energy (Figure 3).

SEM images showed that a periodic structure formed around the craters (outside the regions containing grains), aligned with the polarization plane of the laser radiation. No effect of polarization on the spatial distribution of grains over the surface was detected.

Fourier analysis revealed a periodicity of $\sim 1\,\mu$m at the initial stages of surface structure formation. After 2000 and 10 000 pulses, the periodicity was $\sim 3\,\mu$m. Since the period is comparable to the wavelength, interference may contribute substantially during the initial stage of sample surface damage. A discrete laser interference pattern initially forms on the surface and affects its geometry. This pattern subsequently breaks down as the radiation is scattered by the newly formed surface irregularities, gradually increasing the spatial period. Randomly distributed grains then form, and their size increases with pulse number; periodic surface patterns also appear on the grains themselves. Morphological analysis revealed no systematic features of

Table 2. Geometrical parameters of craters on germanium single-crystal surfaces

Crystallographic orientation of the irradiated plane	(100)	(110)	(111)
10 pulses, 0.1 ms, 0.5 mJ			
Mean crater depth, μm	1.12	0.53(0.76)*	0.43(0.63)
Crater diameter at the surface, μm	100	102	105
Sa of the crater surface, μm	0.121	0.082	0.053
100 pulses, 1 ms, 5 mJ			
Mean crater depth, μm	3.12(1.92)	2.02(0.36)	2.53(0.42)
Crater width at the surface, μm	123	123	120
Sa of the crater surface, μm	0.423	0.165	0.214
300 pulses, 3 ms, 15 mJ			
Mean crater depth, μm	4.31(2.1)	3.11	3.18(1.05)
Crater width at the surface, μm	115	113	123
Sa of the crater surface, μm	0.930	0.341	0.641
500 pulses, 5 ms, 25 mJ			
Mean crater depth, μm	4.20(2.21)	3.36	2.52(1.21)
Crater width at the surface, μm	116	135	118
Sa of the crater surface, μm	0.821	0.581	1.086
700 pulses, 7 ms, 35 mJ			
Mean crater depth, μm	4.21(2.31)	3.67(1.84)	4.46
Crater width at the surface, μm	108	137	109
Sa of the crater surface, μm	0.795	0.449	0.641
1000 pulses, 10 ms, 50 mJ			
Mean crater depth, μm	4.60(1.61)	3.83(2.15)	3.40(2.17)
Crater width at the surface, μm	101	111	112
Sa of the crater surface, μm	0.819	0.780	1.149
2000 pulses, 20 ms, 100 mJ			
Mean crater depth, μm	8.12	6.22(1.89)	6.52
Crater width at the surface, μm	117	112	118
Sa of the crater surface, μm	0.861	1.386	0.869
10 000 pulses, 100 ms, 500 mJ			
Mean crater depth, μm	63.86	51.52	61.13
Crater width at the surface, μm	167	122	129
Sa of the crater surface, μm	5.028	5.426	7.525

Note. * Values in parentheses indicate channel depths.

the grain shapes or in-plane orientations associated with the crystallographic orientation of the sample surface.

4. Conclusion

The surface corresponding to the (100) crystallographic plane was found to be the most susceptible to damage. The surface energies of different Ge facets (plane orientations) differ because of differences in atomic packing density and the number of surface dangling bonds. The (100) plane has the highest surface energy. The experiments revealed no crystallographic features in the surface topography or grain geometry. This is most likely attributable to the short laser pulse duration and, consequently, the absence of the crystallization rate required for oriented structure formation, whether from the vapor phase or from the melt.

Funding

This work used the resources of MISIS and the shared research facilities of Tver State University under the state assignment for research activities (project № 0817-2026-0006) and a Russian Science Foundation grant (Agreement № 24-19-00727).

Conflict of interest

The authors declare that they have no conflict of interest.

References

[1] A.A. Ionin, S.I. Kudryashov, A.A. Samokhin. Phys. Usp., **60** (2), 149 (2017). DOI: 10.3367/UFNe.2016.09.037974
[2] N.A. Inogamov, Y.V. Petrov, V.A. Khokhlov, V.V. Zhakhovskii. High Temperature, **58** (4), 632 (2020). DOI: 10.1134/S0018151X20040045
[3] N.S. Zakharov, S.V. Kholod. *Interaction of ultrashort laser pulses with matter* (12th Central Research Institute, Ministry of Defense of the Russian Federation, Sergiev Posad, 2012) (In Russian).
[4] A.V. Dostovalov. *Fabrication of periodic structures inside optical fibers and on metal surfaces using femtosecond radiation*. Abstract of Cand. Sci. Dissertation (Institute of Automation and Electrometry, Siberian Branch, Russian Academy of Sciences, Novosibirsk, 2014) (In Russian).
[5] I.A. Kaplunov, V.E. Rogalin. Photonics Russian, **13** (1), 88 (2019). DOI: 10.22184/FRos.2019.13.1.88.106
[6] A.A. Ionin, S.I. Kudryashov, A.A. Rudenko, L.V. Seleznev, D.V. Sinitsyn, S.V. Makarov. Optical Mater. Express, **7** (8), 2793 (2017). DOI: 10.1364/OME.7.002793